Chapter 4
Aluminosilicate Inorganic Polymers (Geopolymers): Emerging Ion Exchangers for Removal of Metal Ions

Bassam I. El-Eswed

Abstract Geopolymers (GPs), also known as alkali-activated aluminosilicates or inorganic polymers, are synthesized from an aluminosilicate source (fly ash, metakaolin, or blast furnace slag) and very alkaline sodium hydroxide and/or silicate. Due to their high compressive strength, acid and fire resistance, GPs are used as construction and coating materials. However, since the structure of GP contains negatively charged Al(III) tetrahedra (balanced by alkali cations), they are feasible ion exchangers. The present chapter is aimed to encapsulate the developments in the field of using GPs for the removal of alkali metals (Li^+, K^+, Cs^+), alkaline earth metals (Mg^{2+}, Ca^{2+}, Sr^{2+}, and Ba^{2+}), ammonium ion, and heavy metals (Pb^{2+}, Cu^{2+}, Cd^{2+}, Zn^{2+}, Ni^{2+}, Cr^{3+}) from water. GPs are the first cementing materials that have remarkable ion exchange capacity. GPs have higher ion exchange/adsorption capacity, but a lower rate of adsorption than their precursors (fly ash, metakaolin,…). Thus, geopolymerization increases the adsorption sites on one hand but imposes kinetics limitations that render GPs slow adsorption. GPs resemble zeolites in respect of cation exchange capacity, high surface area, and thermal stability. However, the synthesis of GPs is easier and inexpensive with lower energy and water demand than zeolite synthesis. The prepared GP could be directly formulated as high compressive strength granules at a low temperature. Since GPs are more acid resistant, they are accessible for regeneration than zeolites, but this issue requires further work.

Abbreviations

BET	Brunauer–Emmett–Teller (BET) theory
BFS	Blast furnace slag from iron manufacturing
CEC	Cation exchange capacity (meq/mol)
EDS	Energy-dispersive X-ray spectroscopy
FA	Fly ash from electricity plant employing coal (low calcium, type F)
GP	Geopolymer

B. I. El-Eswed (✉)
Zarqa College, Al-Balqa Applied University, P.O. Box 313, Zarqa 13110, Jordan
e-mail: bassameswed@bau.edu.jo

Inamuddin et al. (eds.), *Applications of Ion Exchange Materials in the Environment*,
https://doi.org/10.1007/978-3-030-10430-6_4

k_2 Pseudo-second-order rate constant (g mg^{-1} min^{-1})
K_L Langmuir affinity constant (L mg^{-1})
MK Metakaolin
Q_m Adsorption capacity (mg g^{-1})
SEM Scanning electron micrographs
XRD X-ray diffraction

4.1 Introduction

The term geopolymer (GP) was first used by Joseph Davidovits in 1978 [1]. GPs, which are also known as alkali-activated materials [2], are synthetic aluminosilicate inorganic polymers which are prepared by reacting a low-calcium solid aluminosilicate with highly basic sodium or potassium hydroxides and silicates at a temperature ranges from 40 to 80 °C [3, 4]. The GPs are used as construction and coating materials [5]. These applications arise from the GPs characteristics which include rapid hardening, compressive strength, low thermal conductivity, stability in acids and fireproof [3, 5–7].

The structure of GP can be represented by a three-dimensional structure of tetrahedral Si(IV) and Al(III) atoms connected covalently by oxygen atoms (Fig. 4.1). Alkali cations (most commonly Na^+ and K^+) are complementary to the GP structure to balance the negative charges of Al(III) tetrahedra [6]. Thus, the structure of GP imposes strongly the property of ion exchange, considering that this property depends to some extent on the porosity of GP [2].

Any aluminosilicate source is suitable, in principle for the preparation of GP. Thus, industrial wastes like fly ash (FA) and blast furnace slag (BFS) obtained from coal electricity plants and metallurgical industries, respectively, could be used

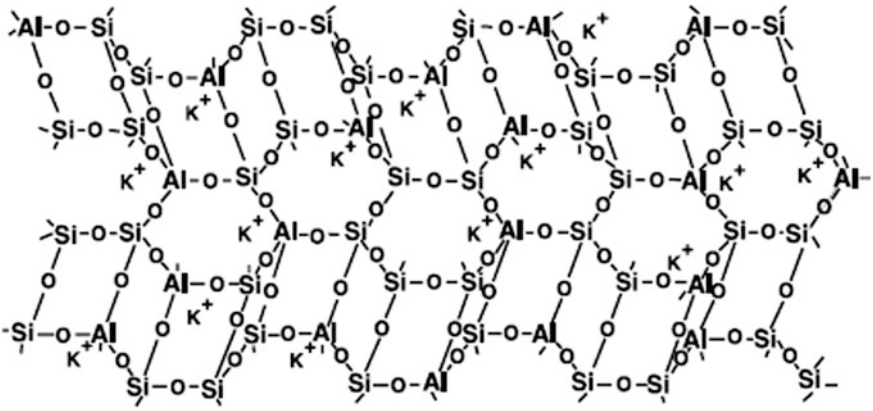

Fig. 4.1 Proposed structure of geopolymer or aluminosilicate inorganic polymer

as source material for GPs. Furthermore, natural aluminosilicates like kaolin and its dehydroxylated product (metakaolin, MK) are suitable for this purpose as well [6]. FA may be the most favored aluminosilicate source for the synthesis of GPs due to the high compressive strength of the GP product and the low water demand [3, 8]. Regarding sustainability, GPs are superior to ordinary Portland cement (OPC) since GPs are produced from inexhaustible sources of wastes using relatively low energy with low CO_2 emissions [6]. The typical stoichiometries for materials used in GP preparation are (in molar ratios): Na/Al = 1, Si/Al = 2, and H_2O/Na $\approx$ 7 [9].

There are two main lines of research for application of GPs in the field of treatment of heavy metals or hazardous wastes. The first is ion exchange/adsorption of heavy metals from an aqueous solution which is the topic of the present chapter. The second is stabilization/solidification/immobilization or encapsulation of heavy metal wastes in GP which involves incorporation of heavy metal waste during the preparation of GP and before hardening of GP paste [10–14]. Stabilization/solidification is a method for waste treatment in which the waste (including heavy metals and water) is encapsulated (as a whole) in the GP cementing material before being finally disposed of in a landfill. Since this immobilization process was assumed to occur via reactions involving precipitation of heavy metals, physical encapsulation, or chemical reactions, it will not be considered in the present chapter except in the cases relevant to ion exchange process.

According to Davidovits, GPs particulates are like those of rock-forming minerals. The OH groups are absent inside the GP network, providing long-term stability and corrosion resistance [15]. GPs are mainly amorphous, even though crystalline zeolitic phases could be embedded in the GP amorphous paste [8].

The aim of the present chapter is to shed some light on the available up-to-date literature in the research area of using GPs in ion exchange/adsorption of alkali, alkaline, and heavy metal ions, as well as ammonium and cationic dyes. These relatively new emerging ion exchangers will be reviewed regarding efficiency in removal of metal ions, kinetics, and mechanism. A comparison of GPs with traditional inorganic ion exchangers like zeolites will be established.

4.2 Methodology and Calculations

4.2.1 Terminology: Ion Exchange or Adsorption

Usually, the occurrence of an ion exchange/adsorption of metal ions on the GP is judged depending on the reduction of the concentration of metal ion in solution. A strict differentiation between ion exchange and adsorption is impossible. Thus, in the present work, the terminology (ion exchange or adsorption) used by the authors of original articles was adopted in the discussion of their works.

4.2.2 Evidence for Ion Exchange

The works which use ion exchange terminology were distinguished in considering not only the ions that are removed from the solutions but also those released from the solid phase (GPs) to achieve electroneutrality. Thus, the differentiation of ion exchange from adsorption processes is guided by the quantification of counterions released during the ion exchange process (Na^+ or K^+ balancing the Al tetrahedra in GPs). Furthermore, in some works, the occurrence of ion exchange was judged by XRF and EDS analyses of the GP after ion exchange where the attachment and release of ions can be evidenced.

4.2.3 Modeling of Adsorption of Metal Ions on Geopolymers

The adsorption experiment is usually carried out by preparing a standard solution of metal solution (C_i) and agitating specific volume (V in L) of this solution with an amount of GP (m, in grams) for a time sufficient to reach equilibrium. The equilibrium time is the time needed to reach a constant concentration of metal in solution (C_e). Then the amount of metal adsorbed (Q_e, mg g^{-1}) is calculated using (4.1).

$$Q_e = \frac{C_i - C_e}{m} V \tag{4.1}$$

Langmuir model (4.2) was used to evaluate the adsorption isotherms published in the articles reviewed:

$$Q_e = \frac{Q_m K_L C_e}{1 + (K_L C_e)} \tag{4.2}$$

where Q_m (mg g^{-1}) represents the efficiency of the GP in removing metal ions from solution, and K_L (L mg^{-1}) is the equilibrium constant used to estimate the affinity of metal toward the surface of GP [16].

Pseudo-second-order rate adsorption constant (k_2, g mg^{-1} min^{-1}) was used to evaluate and compare the kinetics data of articles being reviewed. The pseudo-second-order model is given in (4.3):

$$\frac{dQ_t}{dt} = k_2 (Q_e - Q_t)^2 \tag{4.3}$$

where Q_t and Q_e are the quantities of metal adsorbed at time t and equilibrium time, respectively [17].

4.2.4 Geopolymer Preparation

The preparation conditions of GPs were included in the description of works reviewed. The aluminosilicate source material used in preparation of GP (FA, BFS and MK, kaolin or zeolite) was indicated to give the reader some insight about the effect of variation of source material on the ion exchange behavior of GP. The alkali activator (sodium hydroxide or silicate, potassium hydroxide or silicate), as well as the molar ratios of Si/Al, Na or K/Al, and H_2O/Na, was also given because these are important in estimating the amount of negatively charged Al tetrahedra and the amount of Na^+ or K^+ balancing these negative charges in the GP framework.

4.2.5 Washing of the Geopolymeric Adsorbent

Unless otherwise specified, washing of the prepared GP with distilled or deionized water was carried out before using GP as an ion exchanger/adsorbent. This washing was necessary to avoid overestimation of adsorption capacity that resulted from precipitation of heavy metal ions by reaction of heavy metal ions with unreacted alkali in the GP matrix. Precipitation could not occur in the case of ion exchange or adsorption of alkali metals and ammonium ion on GPs, but washing was also conducted to remove unreacted alkali from the GP. Bortnovsky et al. suggested equilibration of the GPs with NH_4^+ to remove unreacted alkali that is usually hosted in the pores of GP before conduction ion exchange by metal ions [18].

However, Skorina pointed out the fact that over-washing, by analogy with zeolites, must be avoided in order not to replace the easily exchangeable ions like Na^+ or K^+ in the GP with strongly attached H_3O^+ [19]. This replacement may underestimate the ion exchange capacity of GPs. This effect was not taken into consideration in most of the works reviewed below where the GPs adsorbents were washed extensively with distilled water to reach a pH value of 7.

It is worth to mention that the pH increase of synthetic aqueous solutions of heavy metals after contact with GP is pronounced due to the lack of pH buffering capacity in these solutions. However, in the case of well-buffered real wastewater effluents, as well as with acidic industrial wastes, the pH increase is less significant. So there is no need to wash the GP adsorbents before being applied to real wastewater [20].

4.2.6 Comparison Between Geopolymers and Zeolites

In order to understand the feasibility of GPs as ion exchangers, the GPs were compared with traditional inorganic ion exchangers like zeolites regarding the

following properties: synthesis conditions, crystallinity, surface area, porosity, cation exchange capacity, selectivity for metal ions, stability in acidic solutions, thermal stability, mechanical strength, and possibility of regeneration.

4.2.7 Geopolymers as Ion Exchangers

4.2.7.1 Geopolymers as Ion Exchangers for Alkali Metal Ions

Cesium ion (Cs^+) is often found in nuclear waste streams. If the radioisotopes of cesium (^{137}Cs and ^{134}Cs) spread over a wide area, these will continue to radiate for a long time [21]. The immobilization of Cs^+ is challenging due to its high solubility in both alkaline and acidic media [22]. Thus, Cs^+ received special attention in the works devoted to using GPs as ion exchangers for alkali metal ions.

As mentioned in the above introduction, GPs contain negatively charged Al tetrahedra which are balanced by Na^+. The ion exchange of Na^+ ions in the metakaolin (MK)-based GP by Cs^+ was first studied by Bortnovsky et al. to test the accessibility of Na^+ ions in the GP pores. The GP was prepared from MK precursor (43.5% Al_2O_3 and 53.7% SiO_2) and sodium hydroxide and silicate activators with initial molar ratios of Si/Al and Na/Al equal to 1.6 and 1.1, respectively. The prepared GP was first equilibrated with NH_4^+ to remove unreacted alkalis before ion exchange with Cs^+. The EDS analysis indicated that the Na/Al molar ratio changed from 1.1 in the case of Na-GP to 0 upon ion exchange with Cs^+ (1.0 g GP per 100 mL of 0.05 M $CsNO_3$), and the resultant Cs/Al molar ratio was 0.56 [18].

Skorina studied ion exchange of Cs^+ on MK-based GP that was prepared using potassium hydroxide as an alkali activator with initial molar ratios of Si/Al = 2.8, K/Al = 3, and H_2O/Al = 10. The GP was repeatedly washed with deionized water to reach pH 7 (usually 5–7 cycles) before being used in ion exchange. Proton-induced X-ray emission (PIXE) analysis indicated that the K/Al molar ratio changed from 1.02 in the case of K^+-GP to 0 upon exchange with Na^+ and Cs^+, and the resultant Na/Al and Cs/Al molar ratios were 0.77 and 0.61, respectively [19]. The potential use of GPs as ion exchangers for Cs^+ was further confirmed by the study of López et al. which indicated that MK-based GP has higher adsorption selectivity for Cs^+ than heavy metal ions like, Cu^{2+}, Ni^{2+}, Cd^{2+}, Zn^{2+}, and Pb^{2+}. The adsorption capacity (Q_m) of Cs^+ on the GP (initial Si/Al = 2, Na/Al = 0.7) was 43 mg/g and was independent on the increase of ionic strength, indicating that the adsorption occurs via nonelectrostatic mechanism [23].

Lee et al. studied the adsorption of Cs^+ on FA/BFS-based GP. The GP, which was prepared from FA and BFS (4:1 mass ratio) and sodium silicate and sodium hydroxide, was found to contain zeolites (Na-P1, sodalite, faujasite, chabazite) as indicated by XRD pattern. The results indicated that the adsorption capacity of Cs^+ on the GP was small (15.2 mg/g) and the adsorption process was slow as the equilibration time was 24 h. This reflects that large size Cs^+ ion has strong

limitations to diffuse through the pores of the GP [24]. Nevertheless, this equilibration time could be reduced to 30 min by using pulverized samples of the GP.

Despite the ion exchange of Cs^+ on GP, stabilization/solidification was suggested as an alternative strategy for immobilization of Cs^+ in the GP matrix. This was achieved by synthesis of Cs^+ bearing zeolites inside the amorphous GP matrix. Haddad et al. studied the immobilization of Cs^+ in GP prepared from MK, sodium hydroxide, and CsOH keeping $(Na + Cs)/Al_2O_3$ molar ratio equal to 1 and $SiO_2/Al_2O_3 \leq 2$. The type of zeolite found in the GP was dependent on the % Cs in the GP: zeolites A and X in the case of 1% Cs and zeolite F ($CsAlSiO_4 \cdot H_2O$) in the case of 50% Cs. Leaching tests indicated strong binding of Na^+ to zeolites X and A and strong binding of Cs^+ to zeolite F [22]. Similarly, Yuan et al. prepared a ceramic product that contains stabilized Cs^+ in the form of pollucite ($CsAlSi_2O_6$) by reacting MK with a mixture of sodium and cesium hydroxide, with initial molar ratios of $SiO_2/Al_2O_3 = 4$ and $(Na + Cs)/Al_2O_3 = 1$, at 1300 °C [21].

Few studies were reported regarding ion exchange of K^+ and Li^+ on Na^+-GP. Complete exchange of Na^+ in MK-based GP (initial molar ratios $SiO_2/Al_2O_3 = 2.89$, $Na_2O/Al_2O_3 = 0.83$) by K^+ was achieved by agitating the GP (after grinding and without washing) with 0.1 M solution of K^+ as revealed by EDS analysis. A lower exchange capacity was obtained in the case of Li^+ (82%). The XRD patterns of the K^+ and Li^+ exchanged GP products, which were heated to 1100 °C, showed crystalline phases of leucite ($KAlSi_2O_6$) and spodumene ($LiAlSi_2O_6$), compared to nepheline ($NaAlSiO_4$) in the case of original Na^+-GP. This gave strong evidence for the ability of K^+ and Li^+ to replace the Na^+ in the GP matrix [25].

4.2.7.2 Geopolymers as Ion Exchangers for Ammonium Ion

Ammonium removal from municipal wastewater is a great challenge. The commonly used biological nitrification–denitrification process is frequently ineffective and difficult to be controlled, especially at low temperature [20]. The main advantage of using GP for the removal of NH_4^+ is the insignificant dependence on temperature [26]. Complete exchange of the Na^+ in MK-based GP ($SiO_2/Al_2O_3 = 2.89$ and $Na_2O/Al_2O_3 = 0.84$) by NH_4^+ was achieved by agitating the GP (without any treatment other than grinding) with 0.1 M NH_4^+ solution as indicated by EDS analysis [25].

Belchinskaya et al. studied the effect of treatment of an aluminosilicate adsorbent (montmorillonite/zeolite 56.56% SiO_2 and 14.32% Al_2O_3) with NaOH on its ion exchange capacity for NH_4^+. The ion exchange capacity of the alkali (NaOH)-treated aluminosilicate was 74.7 mg NH_4^+/g which is higher than that of untreated and acid (HCl)-activated product. The total number of displaced ions (Na^+, K^+, Ca^{2+}, Mg^{2+}) released from the GP was almost equal to the amount of adsorbed NH_4^+, confirming the ion exchange mechanism [27].

Luukkonen et al. studied the adsorption of NH_4^+ on a granulated GP prepared from MK, sodium hydroxide, and silicate. The granulated GP has a good

compressive strength where the force needed to break the granules was 63.85 N. The GP was found to be effective for removing 90% of NH_4^+ from municipal wastewater when the initial NH_4^+ concentration was 32–40 mg/L at 4 g/L dose of GP and 60 min contact time. Furthermore, the results of a field study demonstrated that a limit of 4 mg/L NH_4^+ could be readily reached after treatment of influent municipal wastewater (initial concentration 15–20 mg/L NH_4^+, 0.2 L/min flow rate, and 2 kg GP granules) [20]. Consequently, the same group of research tried to optimize GP preparation conditions for maximized NH_4^+ adsorption capacity (19.8 mg NH_4^+/g). This optimization was obtained using molar ratios of SiO_2/Al_2O_3 = 2.87, Na_2O/Al_2O_3 = 0.78, H_2O/Na_2O = 22.42. Interestingly, GPs prepared from sodium alkali activators were found to have 27-48% higher NH_4^+ adsorption capacity than those prepared from potassium activators [26].

4.2.7.3 Geopolymers as Ion Exchangers for Alkaline Earth Metals

The first important study on this issue was reported by Uehara et al. in 2009. The authors claimed that a cementitious material exhibited ion exchange. The GP was prepared by mixing fly ash (FA), NaOH or KOH, silica powder, and water (initial Si/Al molar ratio of 1.7). The maximum ions' exchange capacity of Ba^{2+} and Sr^{2+} on Na^+ and K^+-GP was found to increase from 2.5 to 3.0 mmol/g (up to 260 mg Sr^{2+}/L and 410 mg Ba^{2+}/L) with the increase of Na/Al or K/Al molar ratio from 0.4 to 0.8. The amount of Sr^{2+} and Ba^{2+} bound to the surface of GP was approximately equal to the released quantity of Na^+ and K^+ [28]. Furthermore, the Na^+ in MK-based GP (SiO_2/Al_2O_3 = 2.89, Na_2O/Al_2O_3 = 0.84) can be exchanged with Mg^{2+} by agitating the GP (without any treatment other than grinding) with 0.1 M solution of Mg^{2+} as revealed by EDS analysis. The % of Na^+ exchange by Mg^{2+} was 57%, which was lower than that of Pb^{2+}, Cd^{2+}, NH_4^+, K^+, Li^+ [25].

4.2.7.4 Geopolymers as Ion Exchangers for Heavy Metals

Metakaolin-Based Geopolymers

By employing a variety of spectroscopic techniques (UV–Vis–NIR diffuse reflectance and ^{27}Al-NMR spectroscopy), Bortnovsky et al. provided strong evidence for the exchange of Na^+ in MK-based GP by paramagnetic Co(II). Furthermore, EDS analysis indicated that the Na/Al molar ratio changed from 1.1 in the case of Na^+-GP to 0 upon ion exchange with Co(II) and the resultant Co/Al molar ratio was 0.59 [18]. Similarly, O'Connor et al. examined ion exchange of Na^+ in MK-based GP (SiO_2/Al_2O_3 = 2.89, Na_2O/Al_2O_3 = 0.84) by Pb(II), Cd (II), and Ag(I). The EDS analysis revealed that the % exchange was 100% in the case of Ag^+ and Pb^{2+} and 78% in the case of Cd^{2+} [25].

Some results for the adsorption of heavy metals on MK-based GP are shown in Table 4.1. Cheng et al. investigated the adsorption of Pb(II), Cd(II), Cu(II), and Cr

Table 4.1 Langmuir adsorption capacity (Q_m, mg/g), the affinity constant (K_L, L/mg), and pseudo-second-order rate constant (k_2, g mg^{-1} min^{-1}) parameters for adsorption of heavy metal on MK-based GP

Adsorbent	Adsorption conditions	Parameter	Pb(II)	Cu(II)	Cr(III)	Cd(II)	Ni(II)	Zn(II)	References
MK-GP	Ci: 50–300 mg/L, pH 4, Solid/liquid = 1.5 g/L	Q_m	147.1	48.78	19.94	67.57			[29]
		K_L	0.1135	0.025	0.158	0.449			
		k_2	1.8×10^{-5}	2.3×10^{-5}	1.8×10^{-3}	8.3×10^{-5}			
MK-GP	Ci: 50–500 mg/L, pH 5, Solid/liquid = 1.25 g/L	Q_m	63.40	59.22					[23]
		K_L	0.0181	0.0117					
Porous MK-GP	Ci: 100 mg/L, pH 5, Solid/liquid = 1.5 g/L	Q_m	45.1	34.5					[31]
		K_L							
		k_2		3.8×10^{-5}					
Porous MK-GP	Ci: 50 mg/L, pH 5, Solid/liquid = 1.5 g/L	Q_m		52.63					[32]
		K_L		0.1359					
		k_2		2.9×10^{-3}					
MK-GP	Ci: 25–600 mg/L, pH 6.4–7.3, Solid/liquid = 3.2 g/L	Q_m					42.61	74.54	[30]
		K_L					19.6	346	
		k_2					8.4×10^{-3}	3.8×10^{-3}	

MK—Metakaolin, *FA*—Fly ash, *BFS*—Blast furnace slag

(III), on MK-based GP. Depending on the obtained values of Q_m in mg metal/g GP, the following selectivity sequence was determined by the authors:

Pb(II) (147.06) > Cd(II) (67.57) > Cu(II) (48.78) > Cr(III) (19.94). This sequence reflects that ions with a large hydrated ionic radius like Cr(III) have a strong tendency to remain in solution and thus adsorbed weakly on the surface of GP [29]. It is worth to mention that the correct sequence for Q_m values should be in mmol metal/g GP:

Cu(II) (0.768) > Pb(II) (0.710) > Cd(II) (0.6011) > Cr(III) (0.383).

The ionic strength effect on the adsorption of heavy metals on MK-based GP was also studied [23, 30]. Lopez et al. observed that changing the ionic strength does not affect the adsorption of Pb(II) on MK-based GP, which suggests a non-electrostatic mechanism [23]. On the contrary, Kara et al. observed that the removal efficiency of MK-GP decreased from 90.69 to 61.68% for Zn(II) and from 87.65 to 73.90% for Ni(II) as the ionic strength changed from 0.02 to 0.2 M. This behavior was ascribed to the increased competition between electrolyte cations and the heavy metal ions by the increase of ionic strength. This reduction in adsorption removal efficiency of Zn(II) and Ni(II) by increasing ionic strength indicates that the adsorption of these ions on the GP involves electrostatic or outer-sphere surface reactions [30]. Furthermore, for the removal of heavy metal ions from water by MK-based GP, the ion exchange mechanism (outer sphere) seems to be more plausible than specific chemical adsorption (inner sphere) because the adsorption of heavy metals onto MK-based GP was also found to be endothermic [29].

Attempts to increase the adsorption performance (reducing the equilibrium time and increasing the Q_m value) of GPs by increasing the porosity of GP were without success. The porous MK-based GPs were prepared by employing sodium dodecyl sulfate or H_2O_2 foaming agents in the GP mixing design (Si/Al and Na/Al molar ratios equal to 1.6 and 1, respectively). Despite the significant increase in the porosity of GP by this technique, slow adsorption was observed by Tang et al. since the equilibrium time for adsorption of Cu(II) on the porous GP was about 50 h [31]. A similar observation was made by Ge et al. where equilibrium time for the adsorption of Cu(II) on the porous GP was 36 h [32]. The Q_m values of porous GP in the case of Pb(II) and Cu(II) (45.1 and 34.5 mg/g, respectively) were less than that classical MK-based GP (63.4 and 59.2 mg/g, respectively) [31].

As(III) and Sb (III) are found in aqueous solutions in the forms of oxyanionic arsenite/arsenate and antimonite/antimonate, respectively. The study of adsorption of these anions onto MK-based GP was carried out by Luukkonen et al. The obtained Q_m values (0.078 and 0.058 mg/g, respectively) were much lower than those obtained for metal cations (Table 4.1). This confirms that these anions are not amenable for being exchange with the Na^+ or K^+ in the GP [33]. Similarly, Medpeli et al. reported a very low adsorption capacity of 0.950 mg/g for adsorption of $HAsO_4^{2-}$ on MK-based GPs [34].

Fly Ash-Based Geopolymers

Some of the parameters (Q_m, K_L and k_2) obtained for adsorption of heavy metals on fly ash (FA)-based GPs [35–39] are summarized in Table 4.2. It is clear that FA-based GPs are good adsorbents for the removal of heavy metals ions. The adsorption capacity (Q_m) of Cu(II) on GP was much higher than that on the FA precursor, which indicates that geopolymerization process creates new adsorption sites [35]. As calculated from values in Table 4.2, the average adsorption capacity of Cu(II) and the affinity constant K_L are 93 ± 8 and 0.08 ± 0.03 L mg^{-1}, respectively, which indicate that the diversity in FA origin and variability in adsorption experiments hardly affect the values of Q_m and K_L. On the other hand, the kinetics parameters reflect different behavior. The adsorption rate constants (k_2, g mg^{-1} min^{-1}) were of much variability as shown in Table 4.2 [37–39]. Furthermore, the reported equilibrium times for adsorption of heavy metals on FA-based GPs vary from 15 min to 30 h [35–37], which indicate the dependence of the kinetics behavior on the degree of compactness of GPs.

An important study for ion exchange of Pb^{2+} on FA-based GP was reported by Uehara et al. The GP was prepared from FA with Si/Al molar ratio of 1.7. The

Table 4.2 Langmuir adsorption capacity (Q_m, mg/g), the affinity constant (K_L, L/mg), and pseudo-second-order rate constant (k_2, g mg^{-1} min^{-1}) parameters for adsorption of heavy metal on FA-based GP

Adsorbent	Adsorption conditions	Parameter	Cu(II)	Pb(II)	References
FA-GP	Ci: 100-250 mg/L, pH 7, Solid/liquid = 0.15 g/L	Q_m	99		[35]
		K_L	0.13		
		k_2	2.8×10^{-5}		
FA-GP	Ci: 10-140 mg/L, pH 5-6, Solid/liquid = 1.4-2.0 g/L	Q_m	96.84	134.95	[36]
		K_L	0.061	0.0607	
		k_2	0.018		
FA-GP	Ci: 100-1000 mg/L, pH 3, Solid/liquid = 4.0 g/L	Q_m		111.1	[41]
		K_L		0.6429	
		k_2		2.7×10^{-3}	
FA/iron ore tailing-GP	Ci: 100–200 mg/L, pH 6, Solid/liquid = 3.0 g/L	Q_m	113.41		[42]
		K_L	0.073		
	Ci: 100–200 mg/L, pH 5, Solid/liquid = 3.0 g/L	Q_m	100.81		
		K_L	0.069		
	Ci: 100–200 mg/L, pH 4, Solid/liquid = 3.0 g/L	Q_m	79.31		
		K_L	0.064		
FA-GP	Ci: 376 mg/L, Solid/liquid = 5.0 g/L	k_2	0.028		[38]
FA-GP	Ci: 246–2501 mg/L, Solid/liquid = 5.0 g/L	Q_m	68.9		[40]

MK—Metakaolin, *FA*—Fly ash, *BA*—Bottom ash, *BFS*—Blast furnace slag

maximum ion exchange capacities of Na^+ and K^+-GP by Pb^{2+} ranged from 2.5 to 3.0 mmol/g (517.5–621.0 mg/g). The release of Na and K from the GP was less than the adsorption of Pb^{2+}, suggesting that ion exchange is not the only operating mechanism [28].

Mužek et al. investigated removal of Cu(II) and Co(II) using a GP prepared from fly ash (FA), sodium hydroxide, and silicate (initial SiO_2/Al_2O_3 = 4.61, Na_2O/Al_2O_3 = 0.69, and H_2O/Na_2O = 11.19). The Langmuir parameters Q_m and K_L were found to be 68.9 mg/g and 7.2 L/mg for Cu(II), and 50.3 mg/g and 0.7 L/mg for Co (II). By the end of the adsorption process, significant amounts of Na, lesser amounts of Si, and nondetectable amounts of Al were found in the remaining solution, supporting ion exchange mechanism and high stability of GP [40].

The similarity between zeolites and FA-based GPs was claimed by some authors. Muzek et al. [39] noticed the similarity of the adsorption behavior of FA-based GP and zeolite Na-X toward Co(II). The following values reveal also that the adsorption parameters of Pb(II) on FA-based GP are close to those on faujasite [41]:

	FA-GP	Faujasite
Q_m (mg/g)	111.11	142.86
K_L (L/mg)	0.6429	0.2966
k_2 (g mg^{-1} min^{-1})	26.73×10^{-4}	13.5×10^{-4}

The adsorption of heavy metals was found to increase with increasing pH due to a decrease of competition between heavy metal ions and H_3O^+ [36, 41, 42]. The Q_m of Cu(II) increases from 79.31 to 113.41 mg/g with pH increase from 4 to 6 [42].

In many studies, the adsorption of heavy metals on FA-based GPs was found to be endothermic and thus entropy driven (positive values of $\Delta H°$ and positive values of $\Delta S°$). The entropy increase in adsorption process may be due to desolvation of metal ions because of their adsorption on the surface of GP [36, 37, 40, 41].

Zeolite-Based Geopolymers

Zeolites were incorporated into GP preparations for many purposes. The first was to increase the adsorption capacity of GP [43–46]. The second was that GP works as a binder for zeolites powder and consequently enables shaping of zeolites as high mechanical strength spheres, granules, or extrudates which can be used as commercial adsorbents for purification of water [44, 47]. The third was to combine the microporosity of zeolites with the mesoporosity of GPs [47]. However, many of these studies evidenced partial or complete dissolutions of crystalline zeolite in the amorphous GP matrix [43, 45, 46, 48] which indicate the participation of zeolite in the geopolymerization process as an aluminosilicate source.

Some of the parameters for adsorption heavy metals on zeolite-based GP are listed in Table 4.3 [43–45]. El-Eswed et al. studied the adsorption of Pb(II), Zn(II),

Cd(II), and Cu(II) on a GP synthesized from natural zeolite (phillipsite) and natural kaolinite using alkali sodium hydroxide. The adsorption rate constants (k_2) for adsorption of heavy metals on the GP samples were less than those obtained in the case of natural kaolinite (Table 4.3), which indicate that GP pores are less accessible for heavy metals than kaolinite sheets [45]. On the other hand, the Q_m values for adsorption of heavy metals on the zeolite/kaolinite-based GP [61.31 mg/g for Pb(II)] were higher than those obtained in the case of raw natural zeolite (40.19 mg/g) and natural kaolinite (9.61 mg/g) [44]. The following trend was obtained for the adsorption of heavy metals on zeolite/kaolinite-based GP [45]:

	Pb(II)	Zn(II)	Cd(II)	Cu(II)
Q_m (mg/g)	61.31	33.47	30.53	24.18
Q_m (mmol/g)	0.296	0.512	0.272	0.381

Andrejkovicova et al. studied adsorption of Pb(II), Cd(II), Cu(II), Zn(II), and Cr(III) onto MK/zeolite-based GP which synthesized by alkali activation (sodium hydroxide and silicate) of a solid mixture of MK, zeolite (clinoptilolite). Depending on the obtained Q_m in mg/g values, the following sequence was obtained [49]:

Pb(II) (202.72) > Cd(II) (53.99) > Cu(II) (35.71) > Zn(II) (30.79) > Cr(III) (18.02)

However, the sequences for Q_m in mmol/L are:

Pb(II) (0.978) > Cu(II) (0.561) > Cd(II) (0.480) ≈ Zn(II) (0.471) > Cr(III) (0.348)

Al-Zboon et al. used natural zeolitic tuff as a sole precursor for preparation of GP adsorbent. The GP was prepared from zeolitic tuff (phillipsite and chabazite) and 14 M NaOH solution (1:1.25 mass ratio). The maximum adsorption capacity (Q_m) of GP toward Zn(II) was 14.8 mg/g, and the K_L was 0.7 L/mg. The adsorption capacity was pH independent in the range from 5 to 7. The equilibration time was 30 min, and the adsorption process was, as usual, endothermic and entropy driven [46].

4.2.7.5 Geopolymers as Ion Exchangers/Adsorbents for Cationic Organic Dyes

The adsorption of dyes' pollutants on the GP received little attention in the literature. Li et al. investigated adsorption of cationic dyes (methylene blue and crystal violet) on FA-based GP. The adsorption capacity of the GP (31.99 mg MB/g and 40.80 mg CV/g) was much higher than that of the unreacted FA precursor (1.60 mg MB/g and 1.63 mg CV/g), and the rate constant of absorption on the GP (6.25×10^{-5} and 2.28×10^{-5} mg g^{-1} min^{-1}, respectively) was much lower than that on unreacted FA (1.01×10^{-2} and 2.25×10^{-3} mg g^{-1} min^{-1}, respectively). Thus, geopolymerization process generates more sites for adsorption/ion exchange of cationic dyes but decreases the rate of adsorption by restricting the accessibility

Table 4.3 Langmuir adsorption capacity (Q_m, mg/g), the affinity constant (K_L, L/mg), and pseudo-second-order rate constant (k_2, g mg^{-1} min^{-1}) parameters for adsorption of heavy metal on zeolite-based GP

Adsorbent	Adsorption conditions	Parameter	Cu(II)	Pb(II)	Cd(II)	Ni(II)	Zn(II)	References
Phillipsite	Ci: 10–100 mg/L, pH 4, Solid/liquid = 1.0 g/L	Q_m	8.46					[43]
		K_L	0.196					
Kaolin		Q_m	5.98					
		K_L	0.020					
Phillipsite/kaolin-GP		Q_m	12.4					
		K_L	0.413					
Phillipsite	Ci: 10–100 mg/L, pH 4, Solid/liquid = 1.0 g/L	Q_m		72.6				[44]
		K_L		0.253				
Kaolin		Q_m		21.0				
		K_L		0.253				
Phillipsite/kaolin-GP		Q_m		112				
		K_L		0.146				
Phillipsite	Ci: 10–100 mg/L, pH 4, Solid/liquid = 1.0 g/L	Q_m	16.07	40.19	12.77	13.74	8.329	[45]
		K_L	0.123	0.088	11.18		0.3015	
		k_2	1.5×10^{-4}	4.3×10^{-5}	6.8×10^{-5}	4.5×10^{-4}	1.8×10^{-4}	
Kaolin		Q_m	7.212	9.61	8.35	1.607	19.00	
		K_L	0.0783	0.276	14.96		0.0145	
		k_2	5.7×10^{-4}	2.842×10^{-4}	10.4×10^{-3}	2.5×10^{-4}	5.5×10^{-4}	
Phillipsite/kaolin-GP		Q_m	24.18	61.31	30.53	16.63	33.47	
		K_L	0.304	0.1326			0.0593	
		k_2	3.8×10^{-5}	5.05×10^{-5}	8.7×10^{-5}	2.2×10^{-4}	7.6×10^{-5}	

(continued)

Table 4.3 (continued)

Adsorbent	Adsorption conditions	Parameter	Cu(II)	Pb(II)	Cd(II)	Ni(II)	Zn(II)	References
Clinoptilolite/MK-GP	Ci: 20–3000 mg/L, pH 6–7, Solid/liquid = 1.0 g/L	Q_m	35.71	202.72	53.99		30.79	[49]
		K_L	0.337	0.038	0.125		0.483	
Phillipsite/Chabazite-GP	Ci: 10–160 mg/L, pH 7, Solid/liquid = 8.0 g/L	Q_m					14.7	[46]
		K_L					1.26	
Mordenite/MK-GP	Ci: 250 mg/L	Q_m	7.8					[48]

MK—Metakaolin, *FA*—Fly ash, *BA*—Bottom ash, *BFS*—Blast furnace slag

of these sites for large molecular size dyes [50]. The adsorption of methylene blue on zeolite/kaolinite-based GP was similar (26 mg/g) [43]. It is worth to mention that the reactions of methylene blue and crystal violet in highly basic conditions of GP predation conditions need further research since these dyes may undergo hydrolysis reactions [51].

Barbosa et al. studied the adsorption of cationic methyl violet 10B dye on a mesoporous GP which was prepared from MK, rice husk ash (96.68% SiO_2), potassium hydroxide, water, and soybean oil (initial SiO_2/Al_2O_3 molar ratio = 4, K_2O/Al_2O_3 = 2, H_2O/K_2O = 10.4). The BET surface area of the produced GP, pore volume, and pore diameter were 62 m^2/g, 0.36 cm^3/g, and 14.3 nm, respectively, which were higher than those for ordinary GP prepared without oil (27 m^2/g, 0.13 cm^3/g, and 9.1 nm, respectively). Furthermore, the adsorption parameters of the mesoporous GP (Q_m, $K_{L,}$ and k_2 values were 40.25 mg/g, 0.0171 L/mg, and 0.0122 g mg^{-1} min^{-1}, respectively) were higher than those of the ordinary GP for adsorption of methyl violet 10B (Q_m = 13.4 mg/g and k_2 = 0.021 g mg^{-1} min^{-1}, respectively) [52]. Noteworthy, as in the work Li et al. [50], the work of Barbosa et al. indicated that the rate constant k_2 of methyl violet 10B found in the case of unreacted MK (0.01342 g mg^{-1} min^{-1}) was higher than that obtained in the case of MK-based GP (0.01217 g mg^{-1} min^{-1}).

4.2.8 Comparison of Geopolymers with Zeolites

4.2.8.1 Synthesis Conditions

Hydrothermal crystallization of aluminosilicate gel has been used in zeolite synthesis processes for a long time [53]. Zeolites are usually synthesized from aqueous sodium silicate and sodium aluminate in a closed hydrothermal system at a specific temperature, autogenous pressure, and varying time (ranges from few hours to several days) [54]. The time needed to start crystallization of mordenite was reported to increase with a decrease in temperature of crystallization; 4 weeks at 100 °C and 1 h at 350 °C [55]. To be fabricated as pellets or extrudates, the zeolite powder must be mixed with clay and water followed by calcination at 300–600 °C [54]. Thus, synthesis of zeolite requires relatively high energy.

However, the synthesis of zeolite from coal fly ash (FA type F, low calcium) was attempted under mild conditions. Low-silica zeolitic materials (NaP1, A, X, KM, chabazite, and faujasite) were obtained using different conditions of the open or closed system, different NaOH or KOH solutions/fly ash ratios, atmospheric or water vapor pressures, and crystallization time ranged from 3 to 48 h at 80–200 °C [56]. Franus et al. synthesized three types of zeolites from FA by varying the reaction conditions: Na-X (20 g FA per 0.5 L of 3 M NaOH at 75 °C), Na-P1 (20 g FA per 0.5 L of 0.5 M NaOH at 95 °C), and sodalite (20 g FA per 0.8 L of 5 M NaOH and 0.4 L of 3 M NaCl at 95 °C) [57]. Thus, the type of synthetic zeolite

obtained from FA is a function of pH, the concentration of reagents, and temperature [58].

GPs are the amorphous analogues of zeolites because synthesis of both materials can be conducted under hydrothermal conditions. In GP synthesis, the temperature and the amount of water are generally kept lower than those in zeolite synthesis. The temperatures employed in GP synthesis range from 40 to 80 °C, and the water content can be expressed as H_2O/M_2O molar ratios of around 10–20 (M = Na^+ or K^+) [53]. Some of the reported water/FA mass ratios for the preparation of FA-based GP and zeolite were about 0.4 [59, 60] and 30 [57], respectively. Thus, from the economic, energy, and water saving point of views, GPs have been synthesized under better conditions than zeolites.

4.2.8.2 Crystallinity

On the contrary to crystalline zeolites which have definite peaks in their XRD patterns, the GPs are often found to be X-ray amorphous. A "hump" centered at approximately 27–29° 2θ is usually the major characteristic of the XRD pattern of GPs [8]. However, high-resolution microscopy (Fig. 4.2) showed that the GP contains nano-crystalline aluminosilicate particles [53]. In general, longer reaction times in GP synthesis generated more crystalline products embedded in the amorphous GP [53]. Furthermore, GPs prepared using CsOH (as an alkaline activator) were found to contain significant amounts of crystalline zeolites A, X, and F [21, 22].

It is worth to emphasize that activation of MK with alkaline sodium silicate, rather than sodium hydroxide solution, causes rapid nucleation of solid products surrounding the dissolving MK particles and consequently gives geopolymeric rather than highly crystalline zeolitic products [53].

4.2.8.3 Surface Area and Porosity

Franus et al. synthesized three kinds of zeolitic materials from FA: sodalite, Na-P1, and Na-X, with BET specific surface area of 33, 71, and 166 m^2/g, respectively. The textural analysis indicates that sodalite and Na-P1 are mesoporous–microporous, and the Na-X is microporous [57]. The small pore size of sodalite (2.3 Å) renders it low potential application in ion exchange. On the other hand, the larger pore size of Na-X (7.3 Å) makes this zeolite a promising ion exchanger [56].

It is well established that geopolymerization process increases the specific surface area of aluminosilicate source (MK, FA, BFA). Wang et al. reported that geopolymerization resulted in an increase of BET surface area from 8.4 m^2/g in the case of FA to 31.8 m^2/g in the corresponding GP [29]. A similar trend was observed by Li et al. where the surface area increases from 16.45 m^2/g in unreacted FA to 20.48 m^2/g in the FA-based GP [41]. Furthermore, Luukkonen et al. observed that the BET surface area increases from 2.79 and 11.5 m^2/g in case of

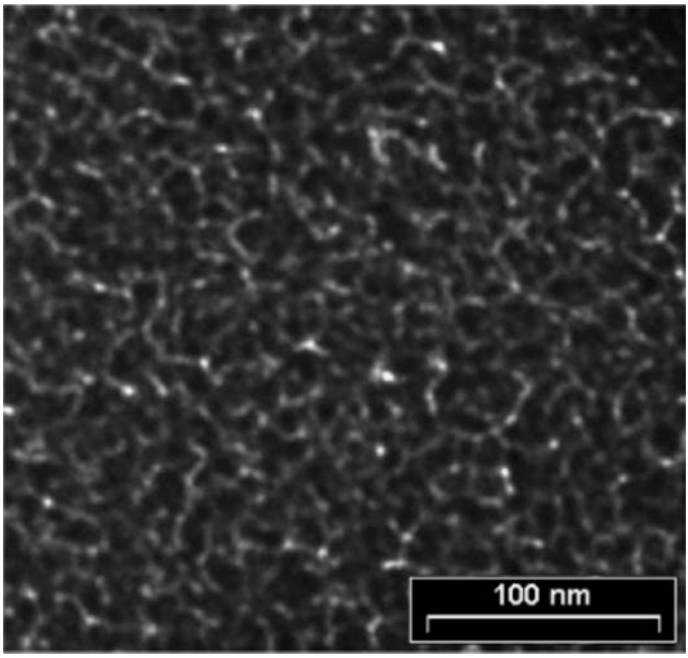

Fig. 4.2 TEM micrograph of a section of MK-based GP [53]. Reprinted with permission from (Provis J. L., Lukey G. C., van Deventer J. S. J. Do Geopolymers Actually Contain Nanocrystalline Zeolites? A Reexamination of Existing Results. Chem. Mater. 2005, 17, 3075–3085). Copyright (2005) American Chemical Society

Table 4.4 Specific surface areas, and volumes of the geopolymers and their raw materials [33]

	BFA	BFS-GP	MK	MK-GP
Specific surface area (m^2/g)	2.79	64.5	11.5	22.4
Marco-mesopore volume (cm^3/g)	0.008	0.070	0.047	0.165
Micropore volume (cm^3/g)	0.001	0.025	0.005	0.008

unreacted BFS and MK, respectively, to 64.5 and 22.4 m^2/g in case of their corresponding GPs (Table 4.4) [33]. The average BET surface area of 34 samples of MK-based GPs prepared using different initial Si/Al and Na or K/Al molar ratios were 50 ± 27 m^2/g, and the average pore size was 22 ± 6 nm (mesoporous) [26].

GPs are macroporous/mesoporous in comparison with microporous zeolites. As evident from Table 4.4, the % macro-mesoporosity values of BFS-GP and MK-GP (74 and 95.4%, respectively) are higher than the % microporosity values (26 and 4.6%, respectively). [33]. For 34 samples of MK-based GPs prepared under different experimental conditions, the % macroporosity, mesoporosity, and microporosity were 31 ± 19, 69 ± 19, and 0.52 ± 0.13, respectively [26].

Table 4.5 Comparison between geopolymers and synthetic zeolites

Aspect of comparison	Geopolymers	Synthetic zeolites
Temperature of synthesis	40–80 °C	100–600 °C
Amount of water used in the synthesis	Low water/FA mass ratio = 0.4 Low H_2O/Na_2O molar ratio = 10–20	High water/FA mass ratio = 20–40 High H_2O/Na_2O molar ratio = 30
Mechanical strength	Low temperature 40-80 °C is enough to obtain a high-strength product	Fragile powder, high temperature 500–600 °C is required to obtain granules or extrudates
Stability in aqueous solutions and thermal stability	Stable	Unstable except in the case of high Si/Al molar
Crystallinity	Amorphous	Crystalline
Porosity	Mesoporous, high pore size distribution	Microporous, low pore size distribution
Specific surface area (m^2/g)	20–70	30–170
CEC (meq/g)	0.1–4	0.5–5

According to several studies, GPs have a wider pore distribution than zeolites [19, 41]. The pore size distribution curve of FA-GP was found to be centered at around 14 nm with a wider distribution than faujasite which was sharp and centered at 4 nm [41]. Furthermore, Skorina observed that the average pore size ranged from 5.7 to 20.7 nm [19].

Many attempts have been made to increase the porosity of GP by employing H_2O_2 and sodium dodecyl sulfate as foaming agents. A porous MK-based GP was found to have a bulk density of 0.79 g/cm^3 and total porosity of 60.3%. The pores of the GP were found to center at about 15 nm, which reflected the presence of plenty of mesopores [31]. As the amount of H_2O_2 increases from 0.30 to 1.2% (w/w), the density of MK/FA-based GP decreases from 0.98 to 0.44 g/cm^3 and the porosity increases from 52.0 to 78.4% [61]. The total porosity of FA/iron ore tailing-based GP ranges from 56.9 to 74.6%. The fraction of pores with diameters larger than 50 nm (macropores) for porous GP was higher than that for reference GP. The pore diameter of the porous GP shifts to higher values with the addition of more H_2O_2 [42]. A general comparison of GPs with synthetic zeolites is presented in Table 4.5.

4.2.8.4 Cation Exchange Capacity

In zeolites, the exchangeable metal cations balance the negative charge on the surface of zeolite pores. This negative charge results from the partial replacement of Si by Al tetrahedra [58]. Thus, synthetic zeolites with low Si/Al molar ratio like

faujasite, chabazite, herschelite, NaP1, and 4A have high cation exchange capacity (CEC). For example, the CEC values of zeolite X and NaP1 are 5.0 and 2.7 meq/g, respectively (ammonium method). These values are higher than those obtained for natural clinoptilolite (1.5–2.0 meq/g) [56]. Franus et al. synthesized zeolites from coal FA, namely, Na-X, Na-P1, and sodalite with CEC 1.8, 0.72, and 0.56 meq/g, respectively (Ba^{2+} method) [57].

The CEC values of GPs are comparable to those of zeolites. Some of the reported CEC values of different GPs are: 0.13 [62], 4.15 [27], 1.1 [26], 2.02 meq/g [24] using NH_4^+ method, and 0.2–0.3 meq/g using Ba^{2+} method [28]. Thus, although GPs are cementitious materials which are characterized by compact structure, they are, like zeolites, good ion exchangers.

4.2.8.5 Selectivity for Metal Ions

In general, the selectivity of cationic exchangers typically increases with increase of charge and ionic size of the exchanging ion: $Th^{4+} > La^{3+} > Ce^{3+} > Ba^{2+} > Sr^{2+} > Ca^{2+} > Co^{2+} > Ni^{2+} > Cu^{2+} > Mg^{2+} > Be^{+2} > Ag^+ > Rb^+ > Cs^+ > K^+ > Na^+ > H^+ > Li^+$ [63]. Similarly, the zeolite ion exchange capacity increases with increasing ionic size. The selectivity sequence of clinoptilolite toward metal ions follows the sequence: $Cs^+ > K^+ > Rb^+ > Na^+ > Li^+$ and $Ba^{2+} > Sr^{2+} > Ca^{2+} > Mg^{2+}$ [64]. The selectivity of clinoptilolite for heavy metals varies somewhat in the literature: Pb (II) > Cd(II) > Cu(II) ≈ Zn(II) [65], Pb(II) > Cd(II) > Cu(II) > Zn(II) [64], and Pb(II) > Cu(II) > Cd(II) ∼ Zn(II) [66, 67].

From a collection of trends discussed in Sect. 3.1, the following sequence can be deduced in the case of ion exchange/adsorption of metal ions on GPs:

$Cs^+ > Cu^{2+} \sim Pb^{2+} > Ba^{2+} > Sr^{2+} > K^+ > NH_4^+ > Li^+ > Cd^{2+} > Mg^{2+} > Na^+$ [23, 25, 26, 28, 29]. Thus, the selectivity sequence of GPs toward metal ions is similar but not identical to those of zeolites. It is worth to mention that the selectivity order changes with the concentration of metal ions in solution and depends on whether it is based on values in mg/g (incorrect) or mmol/g.

4.2.8.6 Stability in Acidic Solutions

The disintegration of zeolites in acidic medium is related to the number of Al atoms, which appear to be the sites of acid attack. Zeolites with high Si/Al molar ratio are stable in acidic medium. Zhuou and Zhu investigated the stability of synthetic zeolites in HCl solution at pH 1 for 3 h by studying their XRD patterns. NaZSM-5 (Si/Al = 12.5–26), NaZSM-11 (Si/Al = 25), Hβ (Si/Al = 14.5), and dealuminated Na-Y (Si/Al = 7) were stable while Na-Y (Si/Al = 2.66) and Na-A (Si/Al = 1) were not and dissolved completely in acidic solutions [68].

Although these have usually Si/Al ratio of about 2, GPs have high acid resistance, and this may be one of the reasons for devoting attention to these materials [69]. Li et al. reported that after 60 days of soaking GP blocks in acetic acid buffer

(pH 3.6), the mass loss of GP was 2.5% [70]. Furthermore, the stability of the GP paste was inferred from the fact that the chemical composition (XRF), especially the % Si and Al, of GP, was not affected by ion exchange process (0.5 g GP/250 ml of 0.1 M $BaCl_2$ and $SrCl_2$) [28].

4.2.8.7 Thermal Stability

Synthetic zeolites like Na-P1, A, X, Y, and P, prepared from FA, have high thermal stability because of their high Si/Al molar ratio. Na-P1, Na-X, and sodalite maintain their crystalline structure at temperatures below 300, 700, and 900 °C, respectively [58]. Similarly, GPs are known to be of excellent thermal stability and already used in fire-resistant coatings, thermal insulation, and furnace linings [71]. After 2 h calcination at 1000 °C, the FA-based GPs can keep a compressive strength of 30 MPa [70].

4.2.8.8 Mechanical Strength

Synthetic zeolites are fragile and often obtained as a powder. These can be fabricated as pellets or extrudates by mixing with a binder like clays followed by calcination at 300–600 °C to get extrudates or granules of sufficient mechanical strength for the purpose of industrial ion exchange processes [54]. On the other hand, GPs as ion exchangers can be formulated as pellets or granules directly during synthesis at 40–80 °C. The compressive strengths of GPs, prepared from FA of different origins, ranged from 30 to 80 MPa [71].

4.2.8.9 Regeneration

Regeneration of the ion exchanger saturated with metal ions results in re-use of the ion exchanger and recovery of metal ions. Thus, the possibility of regeneration has a positive impact on the environment in eliminating the possibility of creating new toxic waste. The adsorption of heavy metals on zeolites was found to be reversible, and thus, the regeneration of zeolite is possible [64]. However, the decrease in adsorption/desorption capacity of clinoptilolite with increasing regeneration cycles was remarkable in the case of removal of Pb(II) and Zn(II) from the water. Successive regeneration cycles using 3 M KCl resulted in more than 50% reduction of adsorption efficiency after 9 and 4 cycles for Pb(II) and Zn(II), respectively [65]. This decrease may be due to the decomposition of clinoptilolite during regeneration.

GPs have been shown to be regenerable in several studies, but a limited number of cycles were investigated. Granules of MK-based GP, which were suitable for continuous column mode for adsorption of ammonium ion, are amenable for multiple regenerations with NaCl/NaOH, although two regeneration cycles

decreased the NH_4^+ removal significantly [20]. However, some studies reported that the adsorption of heavy metals on GP was not reversible. Cheng et al. found that the % desorption of Pb(II), Cd(II), Cr(III), and Cu(II) from GP loaded with maximum amounts of these heavy metals was 5.9, 2.1, 14.7, and 1.9%, respectively [29]. Thus, the possibility of regeneration of GPs, as well as zeolites, is still open to further research.

4.2.9 Stabilization/Solidification/Encapsulation of Ion Exchangers in Geopolymers

An integrated process consists of adsorption followed by solidification/stabilization has been suggested in the literature as a method for encapsulation of exhausted ion exchangers (like fly ash and red mud). For example, heavy metal-loaded fly ash and red mud have been successfully solidified by adding Portland cement producing durable concrete blocks with a compressive strength of 30 MPa [72].

Since alkali-activated aluminosilicates or GPs are alternatives for Portland cement, GPs have been used to encapsulate exhausted ion exchangers. Ipatti investigated encapsulation of exhausted granular boric acid-based ion exchange resins in alkali-activated blast furnace slag (37.7% CaO, 34.4% SiO_2, and 8.4% Al_2O_3). The alkali activation using $Ca(OH)_2$ and NaOH effectively produced GPs containing ion exchanger with compressive strengths varied between 9 and 19 MPa [73].

Kuenzel investigated encapsulation of Cs^+- and Sr^{2+}-loaded clinoptilolite in MK-based GP (initial Si/Al molar ratio of 2, Na/Al = 0.7–1.3, H_2O/Al = 9). The leached Cs^+ and Sr^{2+} concentrations were below the detection limit (5 ppm). Ion exchange of Cs^+ with the charge balancing ions (Na^+) in GP may be the main factor responsible for the immobilization of Cs^+ in the GP matrix. The uptake of Sr^{2+} and Cs^+ of GP per 1 mol of Al was estimated to be 0.4 and 0.2 mol, respectively. The SEM/EDS studies revealed that the high alkalinity of activating solution (sodium hydroxide and silicate) causes dissolution of clinoptilolite containing Cs^+ and Sr^{2+} (in addition to the MK precursor) followed by the bound of these ions to the MK-based GP aluminosilicate phase (see Fig. 4.3) [74].

The reported high compatibility observed between the organic resins and inorganic GP phases [75] is a promising property that makes GPs potential hosts for encapsulation of exhausted organic ion exchangers which may be a subject for future research.

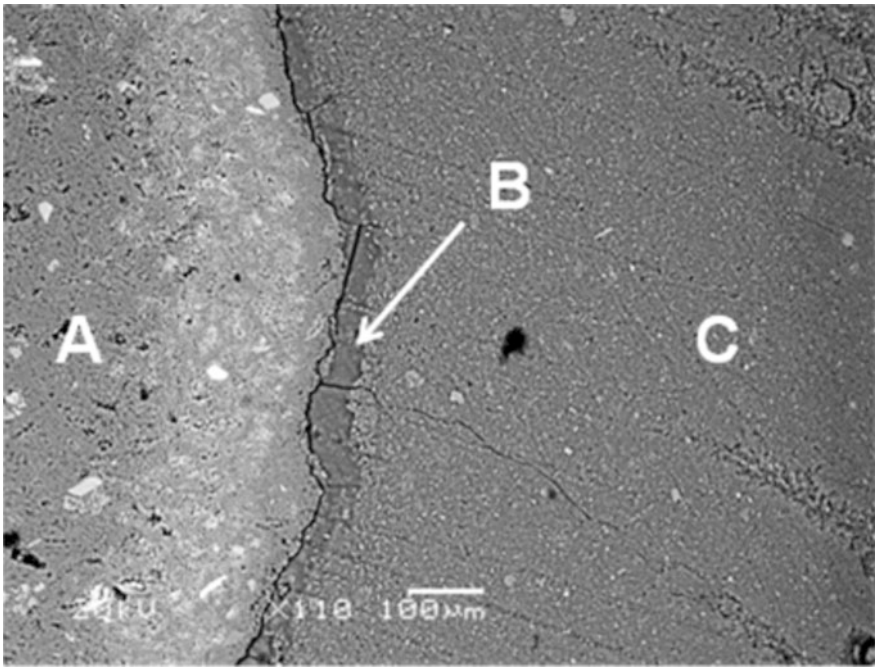

Fig. 4.3 SEM image of MK-based GP used for encapsulation of clinoptilolite containing Cs^+ (A: clinoptilolite, C: MK-based GP, and B: interfacial zone) [74]. Reprinted with permission from (Kuenzel C., Cisneros J.F., Neville T.P., Vandeperre L.J., Simons S.J.R., Bensted J., Cheeseman C.R. Encapsulation of Cs/Sr contaminated clinoptilolite in geopolymers produced from metakaolin. Journal of Nuclear Materials. 2015, 466, 94–99). Copyright (2015) Elsevier B.V

4.3 Concluding Remarks

1. GPs could be used in the treatment of wastewater. The increase in pH of wastewater due to contact with unreacted alkali in GP is expected to be limited due to the buffering capacity of real wastewater and the acidity of industrial wastewater.
2. Despite the high solubility of Cs^+ in water, it could be removed from aqueous solutions using GPs with highly variable adsorption capacity (15–40 mg/g).
3. Complete ion exchange of Na^+ in GP by NH_4^+ was achieved, so GP was applied as an effective ion exchanger for removal of NH_4^+ from real wastewater. The adsorption capacity ranged from 20 to 75 mg/g.
4. Less ion exchange efficiency was obtained in the case of Mg^{2+} and Ca^{2+}.
5. GPs have high ion exchange capacity for Sr^{2+} and Ba^{2+}, as adsorption capacities up to about 250 and 400 mg/g, respectively, were achieved.
6. The adsorption capacities of Pb(II) were 110–130, 50–150, and 60–200 mg/g in the case FA-GP, MK-GP, and zeolite-GP, respectively. On the other hand, the adsorption capacities of Cu(II) were 70–110, 30–50, and 12–36 mg/g,

respectively. These values reflected the strong ability of GPs prepared from various sources for the removal of heavy metals from water.

7. The geopolymerization process results in a remarkable increase in the BET surface area, the adsorption capacity (Q_m), and affinity constant (K_L) relative to starting aluminosilicate precursors (MK and FA). However, the adsorption rate constant (k_2) decreases upon geopolymerization which reflects the slow adsorption rate of heavy metals by GPs due to diffusion limitations in the GP.
8. Increasing the porosity of GPs does not necessarily increase the adsorption capacity and rate constant.
9. The adsorption of ingoing metal ions is associated with the release of outgoing ions. Some interesting features include efficient regeneration of GP adsorbents by NaCl solution, increasing ionic strength and decreasing pH result in a decrease of adsorption, poor adsorption of oxyanions forming metal ions like As(III) and Sb(III) on GPs, and the positive entropy and positive enthalpy of adsorption process (endothermic). Actually, there were no sufficient evidence that support specific chemical bonding of metal ions to the surface of GPs.
10. Exhausted ion exchangers and zeolites (loaded with pollutants) could be encapsulated in GP matrix to give high compressive strength products (with minimum leachability of pollutants). Synthesis of Cs bearing zeolite embedded in the GP matrix is a promising technique for immobilization of Cs^+.
11. GPs have many features that are close to those of zeolites like high cation exchange capacity, high surface area, and thermal stability.
12. The synthesis of GPs is easier because of lower energy and water demand compared to the synthesis of zeolite. The prepared GP could be fabricated directly as high compressive strength granules at low temperature (40–80 °C).
13. Since GPs are more acid resistant than zeolites, GPs are expected to be more stable in the regeneration cycle, but this issue needs further investigations.
14. Zeolites embedded in GPs may be promising materials since they have the advantages of microporous zeolites and meso-/macroporous GPs.
15. GPs are cementing materials as well as ion exchangers which make them multifunctional materials that can serve as a construction material for the removal of pollutants from the environment.
16. The regeneration of exhausted GPs (used in wastewater treatment) and the encapsulation of exhausted zeolites in GP matrix using solidification/stabilization technique are two interesting future research areas.
17. The superiority of GPs to synthetic zeolites in respect of mechanical strength, stability, and cost may be the driving force for using GPs as ionic exchangers in the future.

References

1. Davidovits J (1991) Geopolymers: inorganic polymeric new materials. J Therm Anal 37:1633–1656
2. Provis JL, Fernández-Jiménez A, Kamseu E, Leonelli C, Palom A (2014) Binder chemistry—low-calcium alkali-activated materials. In: Provis JL, van Devente JSJ (eds) Alkali activated materials: state-of-the-art report, RILEM TC 224-AAM, Springer, pp 93–123
3. Ducman V, Korat L (2016) Characterization of geopolymer fly-ash based foams obtained with the. Mater Charact 113:207–213. https://doi.org/10.1016/j.matchar.2016.01.019
4. Melar J, Renaudin G, Leroux F, Hardy-Dessources A, Nedelec J, Taviot-Gueho C, Petit E, Steins P, Poulesquen A, Frizon F (2015) The porous network and its interface inside geopolymers as a function of alkali cation and aging. J Phys Chem C 119(31):17619–17632. https://doi.org/10.1021/acs.jpcc.5b02340
5. Zhang L, Zhang F, Liu M, Hu X (2017) Novel sustainable geopolymer based syntactic foams: an eco-friendly alternative to polymer based syntactic foams. Chem Eng J 313:74–82. https://doi.org/10.1016/j.cej.2016.12.046
6. Zhang Z, Provis JL, Reid A, Wang H (2014) Geopolymer foam concrete: an emerging material for sustainable construction. Constr Build Mater 56:113–127. https://doi.org/10.1016/j.conbuildmat.2014.01.081
7. Zhang F, Zhang L, Liu M, Mu C, Liang YN, Hu X (2017) Role of alkali cation in compressive strength of metakaolin based geopolymers. Ceram Int 43(4):3811–3817. https://doi.org/10.1016/j.ceramint.2016.12.034
8. Duxson P, Fernandez-Jimenez A, Provis JL, Lukey GC, Palomo A, Van Deventer JSJ (2007) Geopolymer technology: the current state of the art. J Mater Sci 42:2917–2933
9. Vance ER, Perera DS (2009) Geopolymers for nuclear waste immobilization. In: Provis JL, Van Deventer JSJ (eds) Geopolymers: structure, processing, properties and industrial applications. CRC Press and Woodhead Publishing Limited, Oxford, pp 401–420
10. Wang Y, Han F, Mu J (2018) Solidification/stabilization mechanism of Pb(II), Cd(II), Mn(II) and Cr(III) in fly ash based geopolymers. Constr Build Mater 160:818–827. https://doi.org/10.1016/j.conbuildmat.2017.12.006
11. Waijarean N, MacKenzie KJD, Asavapisit S, Piyaphanuwat R, Jameson GNL (2017) Synthesis and properties of geopolymers based on water treatment residue and their immobilization of some heavy metals. J. Mater. Sci. 52(12):7345–7359. https://doi.org/10.1007/s10853-017-0970-4
12. El-Eswed BI, Aldagag OM, Khalili FI (2017) Efficiency and mechanism of stabilization/solidification of Pb(II), Cd(II), Cu(II), Th(IV) and U(VI) in metakaolin based geopolymers. Appl Clay Sci 140:148–156. https://doi.org/10.1016/j.clay.2017.02.003
13. El-Eswed BI (2018) Solidification versus adsorption for immobilization of pollutants in geopolymeric materials: a review, solidification. Ares A (ed) InTech. https://doi.org/10.5772/intechopen.72299. Available from: https://www.intechopen.com/books/solidification/solidification-versus-adsorption-for-immobilization-of-pollutants-in-geopolymeric-materials-a-review
14. Al-Mashqbeh A, Abuali S, El-Eswed B, Khalili FI (2018) Immobilization of toxic inorganic anions (Cr2O72-, MnO4- and Fe(CN)63-) in metakaolin based geopolymers: A preliminary study. Ceram Int 44(5):5613–5620. https://doi.org/10.1016/j.ceramint.2017.12.208
15. Davidovits J (2017) Geopolymers: ceramic-like inorganic polymers. J Ceram Sci Technol 08:335–350. https://doi.org/10.4416/JCST2017-00038
16. Foo KY, Hameed BH (2010) Insights into the modeling of adsorption isotherm systems. Chem Eng J 156(1):2–10. https://doi.org/10.1016/j.cej.2009.09.013
17. Tan KL, Hameed BH (2017) Insight into the adsorption kinetics models for the removal of contaminants from aqueous solutions. J Taiwan Inst Chem Eng 74:25–48. https://doi.org/10.1016/j.jtice.2017.01.024

18. Bortnovsky O, Dědeček J, Tvarůžková Z, Sobalík Z, Šubrt J (2008) Metal ions as probes for characterization of geopolymer materials. J Am Ceram Soc 91:3052–3057. https://doi.org/10.1111/j.1551-2916.2008.02577.x
19. Skorina T (2014) Ion exchange in amorphous alkali-activated aluminosilicates: potassium based geopolymers. Appl Clay Sci 87:205–211. https://doi.org/10.1016/j.clay.2013.11.003
20. Luukkonen T, Věžníková K, Tolonen E, Runtti H, Yliniemi J, Hu T, Kemppainen K, Lassi U (2017) Removal of ammonium from municipal wastewater with powdered and granulated metakaolin geopolymer. Environ Technol:1–10. https://doi.org/10.1080/09593330.2017.1301572
21. Yuan J, He P, Jia D, You J, Liu X, Zhang Y, Cai D, Yang Z, Duan X, Wang S, Zhou Y (2017) Effects of Na + substitution Cs + on the microstructure and thermal expansion behavior of ceramic derived from geopolymer. J Am Ceram Soc 100:4412–4424. https://doi.org/10.1111/jace.14968
22. Arbel Haddad M, Ofer-Rozovsky E, Bar-Nes G, Borojovich EJC, Nikolski A, Mogiliansky D, Katz A (2017) Formation of zeolites in metakaolin-based geopolymers and their potential application for Cs immobilization. J Nucl Mater 493:168–179. https://doi.org/10.1016/j.jnucmat.2017.05.046
23. López FJ, Sugita S, Tagaya M, Kobayashi T (2014) Metakaolin-based geopolymers for targeted adsorbents to heavy metal ion separation. J Mater Sci Chem Eng 2:16–27. https://doi.org/10.4236/msce.2014.27002
24. Lee NK, Khalid HR, Lee HK (2017) Adsorption characteristics of cesium onto mesoporous geopolymers containing nano-crystalline zeolites. Microporous Mesoporous Mater 242:238–244. https://doi.org/10.1016/j.micromeso.2017.01.030
25. O'Connor SJ, MacKenzie KJD, Smith ME, Hanna JV (2010) Ion exchange in the charge-balancing sites of aluminosilicate inorganic polymers. J Mater Chem 20:10234–10240. https://doi.org/10.1039/C0JM01254H
26. Luukkonen T, Tolonen E, Runtti H, Kemppainen K, Perämäki P, Rämö J, Lassi U (2017) Optimization of the metakaolin geopolymer preparation for maximized ammonium adsorption capacity. J Mater Sci 16. https://doi.org/10.1007/s10853-017-1156-9
27. Belchinskaya L, Novikova L, Khokhlov V, Tkhi JL (2013) Contribution of ion-exchange and non-ion-exchange reactions to sorption of ammonium ions by natural and activated aluminosilicate sorbent. J Appl Chem:1–9. http://dx.doi.org/10.1155/2013/789410
28. Uehara M, Isogaya S, Yamazaki A (2008) Ion-exchange properties of hardened geopolymers paste from fly ash. Clay Sci 14(3):127–133. https://doi.org/10.11362/jcssjclayscience.14.3_127
29. Cheng TW, Lee ML, Ko MS, Ueng TH, Yang SF (2012) The heavy metal adsorption characteristics on metakaolin-based geopolymer. Appl Clay Sci 56:90–96. https://doi.org/10.1016/j.clay.2011.11.027
30. Kara İ, Yilmazer D, Akar STI (2017) Metakaolin based geopolymer as an effective adsorbent for adsorption of zinc(II) and nickel(II) ions from aqueous solutions. Appl Clay Sci 139:54–63. https://doi.org/10.1016/j.clay.2017.01.008
31. Tang Q, Ge Y, Wang K, He Y, Cui X (2015) Preparation and characterization of porous metakaolin-based inorganic polymer spheres as an adsorbent. Mater Des 88:1244–1249. https://doi.org/10.1016/j.matdes.2015.09.126
32. Ge Y, Cui X, Kong Y, Li Z, He Y, Zhou Q (2015) Porous geopolymeric spheres for removal of Cu(II) from aqueous solution: synthesis and evaluation. J Hazard Mater 283:244–251. https://doi.org/10.1016/j.jhazmat.2014.09.038
33. Luukkonen T, Runtti H, Niskanen M, Tolonen E, Sarkkinen M, Kemppainen K, Ramo J, Lassi U (2016) Simultaneous removal of Ni(II), As(III), and Sb(III) from spiked mine effluent with metakaolin and blast-furnace-slag geopolymers. J Environ Manage 166:579–588. https://doi.org/10.1016/j.jenvman.2015.11.007
34. Medpelli D, Sandoval R, Sherrill L, Hristovski K, Seo D (2015) Iron oxide-modified nanoporous geopolymers for arsenic removal from ground water. Resour-Effi Technol 1 (1):19–27. https://doi.org/10.1016/j.reffit.2015.06.007

35. Wang S, Li L, Zhu ZH (2007) Solid-state conversion of fly ash to effective adsorbents for Cu removal from wastewater. J Hazard Mater 139(2):254–259. https://doi.org/10.1016/j.jhazmat.2006.06.018
36. Al-Zboon K, Al-Harahsheh MS, Bani Hani F (2011) Fly ash-based geopolymer for Pb removal from aqueous solution. J Hazard Mater 188:414–421. https://doi.org/10.1016/j.jhazmat.2011.01.133
37. Al-Harahsheh MS, Al Zboon K, Al-Makhadmeh L, Hararah M, Mahasneh M (2015) Fly ash based geopolymer for heavy metal removal: A case study on copper removal. J Environ Chem Eng 3(3):1669–1677. https://doi.org/10.1016/j.jece.2015.06.005
38. Mužek MN, Svilović S, Zelić J (2013) Fly ash-based geopolymeric adsorbent for copper ion. Desalin Water Treat 52:2519–2526. https://doi.org/10.1080/19443994.2013.792015
39. Mužek MN, Svilović S, Zelić J (2016) Kinetic studies of cobalt ion removal from aqueous solutions using fly ash-based geopolymer and zeolite NaX as sorbents. Sep Sci Technol 51(18):2868–2875. https://doi.org/10.1080/01496395.2016.1228675
40. Muzek MN, Svilovic S, Ugrina M, Zelic J (2016) Removal of copper and cobalt ions by fly ash-based geopolymer from. Desalin Water Treat 57:10689–10699. https://doi.org/10.1080/19443994.2015.1040077
41. Liu Y, Yan C, Zhang Z, Wang H, Zhou S, Zhou W (2016) A comparative study on fly ash, geopolymer and faujasite block for Pb removal from aqueous solution. Fuel 185:181–189. https://doi.org/10.1016/j.fuel.2016.07.116
42. Duan P, Yan C, Zhou W, Ren D (2016) Development of fly ash and iron ore tailing based porous geopolymer for removal of Cu(II) from wastewater. Ceram Int 42(12):13507–13518. https://doi.org/10.1016/j.ceramint.2016.05.143
43. Yousef RI, El-Eswed B, Alshaaer M, Khalili F, Khoury H (2009) The influence of using Jordanian natural zeolite on the adsorption, physical, and mechanical properties of geopolymers products. J Hazard Mater 165:379–387. https://doi.org/10.1016/j.jhazmat.2008.10.004
44. El-Eswed B, Yousef RI, Alshaaer M, Khalili F, Khoury H (2009) Alkali solid-state conversion of kaolin and zeolite to effective adsorbents for removal of lead from aqueous solution. Desalin Water Treat 8:124–130. https://doi.org/10.5004/dwt.2009.672
45. El-Eswed B, Alshaaer M, Yousef RI, Hamadneh I, Khalili F (2012) Adsorption of Cu(II), Ni(II), Zn(II), Cd(II) and Pb(II) onto Kaolin/Zeolite based- geopolymers. Adv Mater Phys Chem 2:119–125. https://doi.org/10.4236/ampc.2012.24B032
46. Alzboon K, Al Smadi B, Al-Khawaldh S (2016) Natural volcanic tuff-based geopolymer for Zn removal: adsorption isotherm, kinetic, and thermodynamic study. Water Air Soil Pollut:227–248. https://doi.org/10.1007/s11270-016-2937-5
47. Papa E, Medri V, Amari S, Manaud J, Benito P, Vaccari A, Landi E (2018) Zeolite-geopolymer composite materials: production and characterization. J Clean Prod 171:76–84. https://doi.org/10.1016/j.jclepro.2017.09.270
48. Alshaaer M, Zaharaki D, Komnitsas K (2014) Microstructural characteristics and adsorption potential of a zeolitic tuff–metakaolin geopolymer. Desalin Water Treat 56(2):338–345. https://doi.org/10.1080/19443994.2014.938306
49. Andrejkovičov S, Sudagar A, Rocha J, Patinha C, Hajjaji W, Ferreira da Silva E, Velosa A, Rocha F (2016) The effect of natural zeolite on microstructure, mechanical and heavy metals adsorption properties of metakaolin based geopolymers. Appl Clay Sci 126:141–152. https://doi.org/10.1016/j.clay.2016.03.009
50. Li L, Wang S, Zhu Z (2006) Geopolymeric adsorbents from fly ash for dye removal from aqueous solution. J Colloid Interface Sci 30(1):52–59. https://doi.org/10.1016/j.jcis.2006.03.062
51. Mills A, Hazafy D, Parkinson J, Tuttle T, Hutchings MG (2011) Effect of alkali on methylene blue (C.I. Basic Blue 9) and other thiazine dyes. Dyes Pigm 88(2):149–155. https://doi.org/10.1016/j.dyepig.2010.05.015
52. Barbosa TR, Foletto EL, Dotto GL, Jahn SL (2018) Preparation of mesoporous geopolymer using metakaolin and rice husk ash as synthesis precursors and its use as potential adsorbent

to remove organic dye from aqueous solutions. Ceram Int 44:416–423. https://doi.org/10.1016/j.ceramint.2017.09.193
53. Provis JL, Lukey GC, van Deventer JSJ (2005) Do geopolymers actually contain nanocrystalline zeolites? A reexamination of existing results. Chem Mater 17:3075–3085. https://doi.org/10.1021/cm050230i
54. Schmidt W (2012) Synthetic inorganic ion exchange materials. In: Inamuddin, Luqman M (eds) Ion exchange technology I. Theory and materials. Springer, pp 277–298
55. Bajpai PK (1986) Synthesis of mordenite type zeolite. Zeolites 6:2–8
56. Querol Carceller X, Moreno N, Alastuey A, Juan Mainar R, Andres Gimeno JM, Lopez-Soler Á, Ayora C, Medinaceli A, Valero A (2007) Synthesis of high ion exchange zeolites from coal fly ash. Geologica Acta 5(1):49–57. http://dx.doi.org/10.1344/105.000000309
57. Franus W, Wdowin M, Franus M (2014) Synthesis and characterization of zeolites prepared from industrial fly ash. Environ Monit Assess 186:5721–5729. https://doi.org/10.1007/s10661-014-3815-5
58. Jha B (2016) Basics of zeolites. In: Jha B, Singh DN (eds) Fly ash zeolites: innovations, applications, and directions, advanced structured materials. Springer. https://doi.org/10.1007/978-981-10-1404-8_2
59. Van Jaarsveld JGS, Van Deventer JSJ, Schwartzman A (1999) The potential use of geopolymeric materials to immobilise toxic metals: part II. Material and leaching characteristics. Mineral Eng 12(1):75–91. https://doi.org/10.1016/S0892-6875(98)00121-6
60. Van Jaarsveld JGS, Van Deventer JSJ (1999) The effect of metal contaminants on the formation and properties of waste-based geopolymers. Cem Concr Res 29:1189–1200. https://doi.org/10.1016/S0008-8846(99)00032-0
61. Novais RM, Buruberri LH, Seabra MP, Labrincha JA (2016) Novel porous fly-ash containing geopolymer monoliths for lead adsorption from wastewaters. J Hazard Mater 318:631–640. https://doi.org/10.1016/j.jhazmat.2016.07.059
62. Buic Z, Zelić B (2009) Application of clay for petrochemical wastewater pretreatment. Water Qual Res J Can 44:399–406
63. Nasef MM, Ujang Z (2012) Introduction to ion exchange processes. In: Inamuddin, Luqman M (eds) Ion exchange technology I. Theory and materials. Springer, pp 1–40
64. Margeta K, Logar NZ, Siljeg M, Farkas A (2013) Natural zeolites in water treatment—how effective is their use, water treatment. In: Dr. Elshorbagy W (ed) InTech. https://doi.org/10.5772/50738. Available from: https://www.intechopen.com/books/water-treatment/natural-zeolites-in-water-treatment-how-effective-is-their-use
65. Katsou E, Malamis S, Tzanoudaki M, Haralambous KJ, Loizidou M (2011) Regeneration of natural zeolite polluted by lead and zinc in wastewater treatment systems. J Hazard Mater 189 (3):773–786. https://doi.org/10.1016/j.jhazmat.2010.12.061
66. Cincotti A, Mameli A, Locci AM, Orrù R, Cao G (2006) Heavy metals uptake by Sardinian natural zeolites: experiment and modeling. Ind Eng Chem Res 45(3):1074–1084. https://doi.org/10.1021/ie050375z
67. Sprynskyy M, Buszewski B, Terzyk AP, Namieśnik J (2006) Study of the selection mechanism of heavy metal (Pb2 + , Cu2 + , Ni2 + , and Cd2 +) adsorption on clinoptilolite. J Colloid Interface Sci 304(1):21–28. https://doi.org/10.1016/j.jcis.2006.07.068
68. Zhou CF, Zhu JH (2005) Adsorption of nitrosamines in acidic solution by zeolites. Chemosphere 58(1):109–114. https://doi.org/10.1016/j.chemosphere.2004.08.056
69. Abora K, Beleña I, Bernal SA, Dunster A, Nixon PA, Provis JL, Tagnit-Hamou A, Winnefeld F (2014) Durability and testing—chemical matrix degradation processes. In: Provis JL, van Devente JSJ (eds) Alkali activated materials: state-of-the-art report, RILEM TC 224-AAM. Springer, pp 177–221
70. Li Q, Sun Z, Tao D, Xu Y, Li P, Cui H, Zhai J (2013) Immobilization of simulated radionuclide 133Cs + by fly ash-based geopolymer. J Hazard Mater 262:325–331. https://doi.org/10.1016/j.jhazmat.2013.08.049

71. Bernal SA, Krivenko PV, Provis JL, Puertas F, Rickard WDA, Shi C, Van Riessen A (2014) Other potential applications for alkali-activated materials. In: Provis JL, van Devente JSJ (eds) Alkali Activated materials: state-of-the-art report, RILEM TC 224-AAM. Springer, pp 339–379
72. Hizal J, Tutem E, Guclu K, Hugul M, Ayhan S, Apak R, Kilinckale F (2013) Heavy metal removal from water by red mud and coal fly ash: an integrated adsorption–solidification/stabilization process. Desalin Water Treat 51:7181–7193. https://doi.org/10.1080/19443994.2013.771289
73. Ipatti A (1992) Solidification of ion-exchange resins with alkali-activated blast-furnace slag. Cem Concr Res 22:281–286. https://doi.org/10.1016/0008-8846(92)90066-5
74. Kuenzel C, Cisneros JF, Neville TP, Vandeperre LJ, Simons SJR, Bensted J, Cheeseman CR (2015) Encapsulation of Cs/Sr contaminated clinoptilolite in geopolymers produced from metakaolin. J Nucl Mater 466:94–99. https://doi.org/10.1016/j.jnucmat.2015.07.034
75. Ferone C, Roviello G, Colangelo F, Cioffi R, Tarallo O (2013) Novel hybrid organic-geopolymer materials. Appl Clay Sci 73:42–50. https://doi.org/10.1016/j.clay.2012.11.001